Bull. Mater. Sci. (2022)45:155
https://doi.org/10.1007/s12034-022-02735-z

Influence of Ca species on the surface properties of TiO_2 nanoparticles and its possible transformation

HASAN SAYGIN[1] and ASLI BAYSAL[2,*]

[1]Application and Research Center for Advanced Studies, T. C. Istanbul Aydin University, Istanbul 34295, Turkey
[2]Health Services Vocational School of Higher Education, T. C. Istanbul Aydin University, Istanbul 34295, Turkey
*Author for correspondence (aslibaysal@aydin.edu.tr)

MS received 21 January 2022; accepted 19 April 2022

Abstract. Metal oxide (e.g., TiO_2) nanoparticles have been used in various environmental, food and medical products. Other chemical species, e.g., major cationic or anionic compounds, are also found in these applications. However, limited information on the interactions of nanoparticles with the other chemical species is available. Thus, this study aimed to examine interaction of TiO_2 nanoparticles with individual and combined presence of Ca compounds by the surface chemistry of TiO_2 nanoparticles using dynamic light scattering, Fourier transform infrared spectrometry and energy-dispersive X-ray spectroscopy. Moreover, surface characteristics such as crystallinity, functional group indices (hydroxyl, carbonyl and vinyl), oxygen to carbon ratio, as well as the influence of surface characteristics on the zeta potential and particle sizes were evaluated. The results indicated that the crystallinity, oxygen to carbon ratio, hydroxyl and vinyl groups of TiO_2 nanoparticles were significantly affected from the interaction with Ca compounds. As a result of surface transformation, affecting the functional groups and crystallinity, the zeta potential and particle size were significantly influenced.

Keywords. Chemical interaction; calcium; nanoparticles; surface chemistry; interference.

1. Introduction

Metal oxide nanoparticles, like TiO_2, have been broadly applied as a promising material for the industrial and domestic applications because of its high efficiency, non-toxicity and chemical stability [1,2]. In these applications, the media include not only the intended nanoparticles but also other chemical species, especially major cationic or anionic species. Moreover, it is known that the occurrence, stability, agglomeration and toxicity of particles can affect from co-species in the media [1,3–9]. For example, Horie *et al* [10] investigated the Ca adsorption on various metal oxide nanoparticles and its effect on cytotoxicity. The study showed that the Ca adsorption ability of ZnO nanoparticles influenced the toxicity. Additionally, the interaction between particles and other chemical species has been evaluated in several studies, specifically in the environmental studies [11–19]. For instance, surface-modified nano zero-valent iron was investigated under the influence of Ca ions in the form of $CaCl_2$, and the sedimentation properties were affected by Ca ions [17]. Tan *et al* [18] examined the effect of magnesium and humic acid on the morphology and aggregation properties of silica aerogels. The results showed that the presence of magnesium as $MgCl_2$ influenced the aggregation of the particles. Similarly, fullerene and boron nanoparticles easily agglomerated at a high concentration in the presence of Ca (as a form of $CaCl_2$) and humic acid [16]. In another study by Baalousha *et al* [19], the influence of monovalent and divalent cations, anions and fulvic acid on the aggregation of citrate-coated silver nanoparticles was investigated. The results showed that divalent cations, compared to monovalent cations, influence the aggregation of nanoparticles [19]. In these studies, experiments were designed using one form of tested co-chemicals. However, the media simultaneously includes many chemical compounds, and mostly these co-chemicals found as salts, such as chloride, sulphates and carbonates, together in the realistic conditions. Moreover, one of the most abundant dissolved ions in the aqueous systems is Ca species and Ca^{2+} often find together in the media as chloride, carbonate, sulphate, etc. Besides, anionic part of the compounds is present in much smaller amounts than the cation part, but they have a vital role in the natural systems [20,21]. Therefore, reflection of the relevant chemical compounds together is important to understand the fate of nanoparticles in the natural systems [22]. Another issue in this field is the necessity of the mimicking of the natural concentrations of the co-chemicals [13,15,18–28], as many

Supplementary Information: The online version contains supplementary material at https://doi.org/10.1007/s12034-022-02735-z.

Published online: 04 August 2022

properties (sedimentation, functionalization, aggregation, etc.) of nanoparticles rely on the concentration dependency [29–31]. In addition, concentration of the co-chemicals are varied according to where they occur; for example, in environmental components, seawater, river water, drinking water, etc., includes different levels of Ca content. Consequently, the studies that examine the effect of co-chemicals on the particles can be reflecting the realistic (environmental) conditions by the species and their concentrations for accurate evaluation.

Furthermore, surface chemistry plays a significant role in the material science, especially their applications, interactions and fate because surface composition dictates the performance and activity of nanoparticles [4–7,32]. However, the surface characteristics of the particles with the interaction of medium components have limitedly detailed [29]. Some important surface characteristics of the particles are crystallinity, functional group indices and oxygen to carbon (O/C) ratio. The crystallinity has an impact on the oxidant generation of particles, and in most cases, decreases in crystallinity hinder molecular motion and increase the formation of free radicals [33]. The functional group indices, such as hydroxyl, carbonyl and vinyl, may be also the most useful tools to determine the surface deformation or transformation due to their easy and ready identification and comparison [34]. The O/C is used to show the degree of oxidation at the surface of materials [35]. Furthermore, in various studies, surface deformation or transformation of polymer was examined using these characteristics, and polymer particles and metal oxide nanoparticles have strong similarities based on their particulate nature [17]. However, the surface deformation, loss or change in functionality of metal oxide nanoparticles is mostly ignored in their studies of aggregation, stability and sedimentation.

Therefore, the present study characterized the surface transformation of TiO_2 nanoparticles in the presence of various individual and combined Ca compounds. For this purpose, the surface characteristics of TiO_2 nanoparticles investigated in terms of the functional group index (hydroxyl, carbonyl and vinyl), crystallinity, O/C, zeta potentials and particle size of TiO_2 NPs evaluated. To examine the interaction with Ca compounds under realistic conditions, we have selected the environmental application of TiO_2 nanoparticles and mimicked the environmentally relevant conditions, like seawater, river water and drinking water.

2. Materials and methods

Solutions of each single Ca compound ($CaCl_2$, $CaCO_3$, $CaSO_4$) and their combinations ($CaCO_3$+$CaCl_2$, $CaSO_4$+$CaCl_2$, $CaCO_3$+$CaSO_4$, $CaCO_3$+$CaSO_4$+$CaCl_2$) were prepared at three Ca concentrations (0.1, 0.01 and 0.001 M, mimicking the concentration of Ca^{2+} in seawater, river water and freshwater) by using ultrapure water at room temperature. The concentration of Ca and other compounds with each treatment are listed in supplementary table 1. TiO_2 nanoparticles (anatase, Nanografi-Turkey) were mixed with each solution at a concentration of 100 mg l^{-1} for 24 h at 250 rpm (pH = 7.0 ± 0.2). After 24 h, the supernatant was removed, and the bulk samples were washed and dried [4,5]. Then, the structural properties of the control and treated TiO_2 particles were analysed. The experimental conditions, such as exposure duration, and nanoparticle concentration were adapted in our previous studies [4,5]. The control of the nanoparticles were without any treatment, and previously dried at 90°C [4,5].

The structural properties (particle size, zeta potentials, surface functionality and elemental composition) of TiO_2 particles were measured using dynamic light scattering (DLS), Fourier transform infrared spectrometry (FTIR) and scanning electron microscopy with energy-dispersive X-ray spectroscopy (SEM/EDX).

The FTIR in conjunction with ATR was carried out using a Bruker VERTEX 70 ATR instrument. The bulk was analysed within the 4000–400 cm^{-1} range. Three likely areas in the spectrum were identified, and related indices were calculated according to the studies of Brandon *et al* [33] and Stark and Matuana [34]. The regions at 1550–1850 cm^{-1}, 3300–3400 cm^{-1} and 871 cm^{-1} are the spectral ranges of carbonyl bonds, hydroxyl groups and vinyl groups. The hydroxyl, carbonyl and vinyl group indices were measured as the ratio of the maximum transmittance of the bond peak to the value of a reference peak. Between 2908 and 2920 cm^{-1}, peaks were selected as the reference peaks for carbonyl bonds, hydroxyl groups and vinyl groups. The results of the functional groups were discussed as relative intensity.

Crystallinity was quantified according to the method described in Brandon *et al* [33] and Stark and Matuana [34]. The doublet peaks observed at 1474–1464 and 730–720 cm^{-1} corresponded to crystalline (1474 and 730 cm^{-1}) and amorphous (1464 and 720 cm^{-1}) contents, respectively. The crystalline content as a percentage was calculated as follows:

$$X = 100-\{[(1-I_c/I_a)/1.233]/(1+I_c/I_a)\},$$

where I_c is the band of crystalline content, I_a is the band of amorphous content and 1.233 is the theoretical intensity ratio for I_c/I_a at a set angle of 42°.

The elemental composition of untreated and treated TiO_2 particles were characterized using an SEM/EDX spectrometer (QUANTA FEG 250, FEI, Thermo Fisher Scientific, Oregon, USA). The O/C ratio was calculated from the EDX spectra.

The particle size and zeta potential were measured via DLS using Zetasizer Nano ZS instruments (Malvern, UK) at 25°C at a scattering angle of 173° using a 4 mW He-Ne laser. Control and treated TiO_2 particles were sonicated for 5 min and placed in standard zeta potential disposable

capillary cells and polystyrene cuvettes for zeta potential and size measurements, respectively.

The differences between control and samples, as well as the differences among samples, were analysed by ANOVA with post hoc Tukey ($p < 0.05$). SPPS 17.0 software was applied for the significance and Spearman correlation (two-tailed, $p < 0.05$) tests.

3. Results and discussion

Fourier transform infrared (FTIR) spectroscopy was employed for the characterization of TiO_2 nanoparticles to specify the possible functional groups present after the treatment of various Ca compounds, shown in figure 1. It can be observed that untreated TiO_2 nanoparticles showed

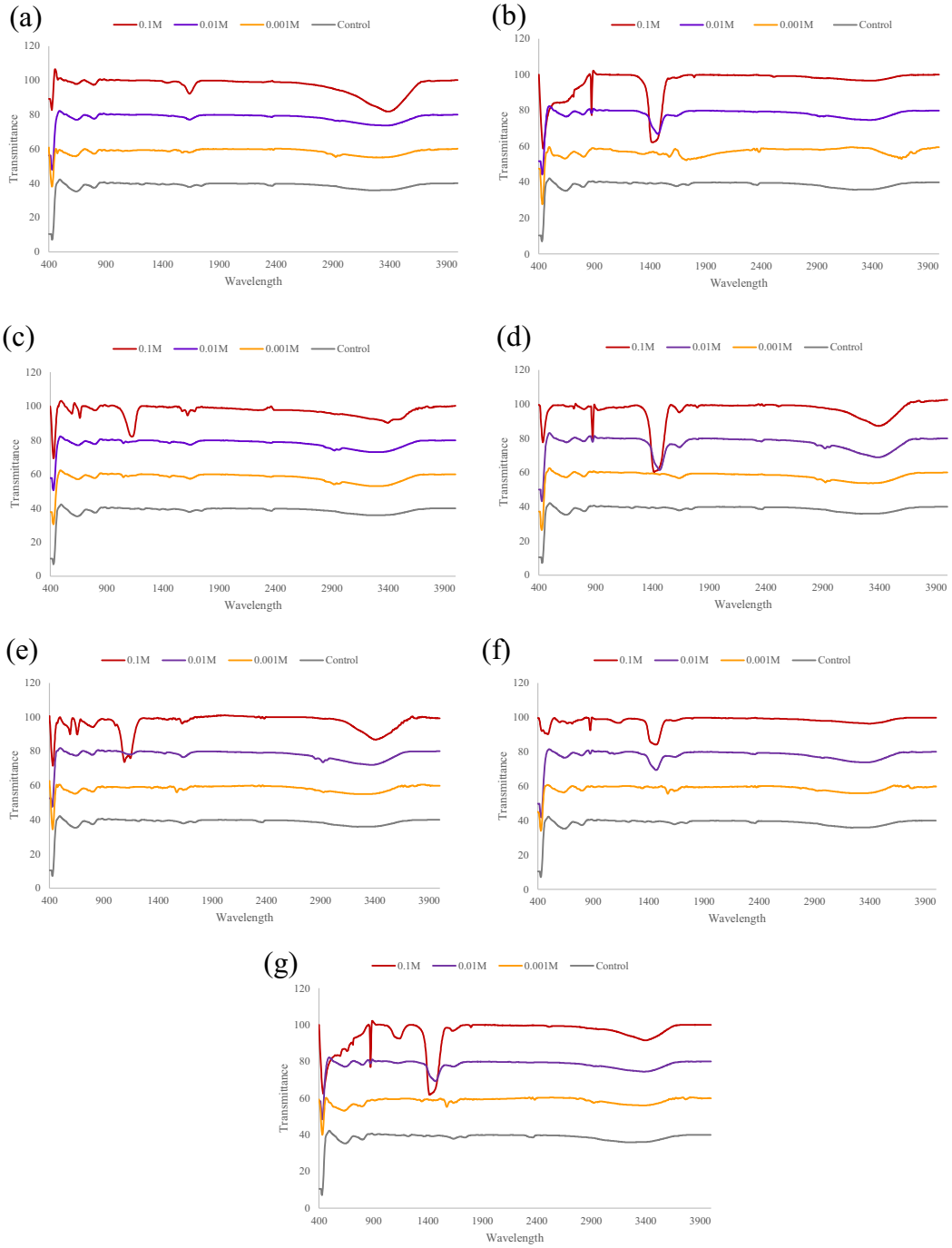

Figure 1. FTIR spectra of TiO_2 particles treated with individual and combined Ca compounds using various concentrations. The treatments are indicated as (**a**) $CaCl_2$, (**b**) $CaCO_3$, (**c**) $CaSO_4$ and their combinations (**d**) $CaCO_3 + CaCl_2$, (**e**) $CaSO_4 + CaCl_2$, (**f**) $CaCO_3 + CaSO_4$, (**g**) $CaCO_3 + CaSO_4 + CaCl_2$.

an absorption band at 790 cm^{-1}, which can be ascribed to Ti–O–Ti stretching. The absorption peak appearing between 620 and 750 cm^{-1} can be attributed to the characteristic peak of TiO_2 anatase phase as reported in literature [36,37]. These characteristic Ti peaks can also be identified in all the spectrums after all the Ca treatments of TiO_2 nanoparticles. Figure 1a indicated that the slight peaks between the range of 1600–1700 cm^{-1} and 2350–2400 cm^{-1} disappeared after the treatment at lowest concentration (0.001 M) of $CaCl_2$. In the increasing concentration of $CaCl_2$ treatment, the peaks appearing within 1645 and 3100–3600 cm^{-1} can be associated with the C=C and –OH. The intensity of –OH groups increased on the surface of TiO_2 with the increasing concentration of $CaCl_2$ treatment. Figure 1b shows FTIR spectra of the TiO_2 with the treatment of various concentrations of $CaCO_3$. The peak is observed in the region of 850 cm^{-1} and at around 1400 cm^{-1} represented the carbonates and the specific carbonate peaks were getting strong with the increasing concentration of $CaCO_3$ (0.01 and 0.1 M). Similar to the $CaCl_2$ treatments, the slight peaks between the range of 1600–1700 and 2350–2400 cm^{-1} disappeared with the treatment of $CaCO_3$. FTIR spectra of TiO_2 treated with the various concentrations of $CaSO_4$ are displayed in figure 1c. The peaks at 600–660, 1400–1600 and 3400–3500 cm^{-1} correspond to the sulphate characteristic peaks. These observations are significant especially at the highest concentration (0.1 M) of $CaSO_4$. FTIR analysis is also carried out to identify the functional groups in the treatments of TiO_2 particles with the double combinations of Ca compounds (figure 1d–f). In the double combination of $CaCO_3$ + $CaCl_2$, the peaks at 1645 and 3100–3600 cm^{-1} attributing with the C=C and –OH of $CaCl_2$ treatment and the absorption peak locating at around 850 and 1400 cm^{-1} identified the carbonates. Although these results were observed at increasing concentration of $CaCO_3$ + $CaCl_2$, which are 0.01 and 0.1 M, the specific peaks originating $CaCl_2$ also appeared with the lowest concentration of the treatment (figure 1d). The FTIR analysis of double combination of the treatment of $CaSO_4$ + $CaCl_2$ is illustrated in figure 1e, the peaks are observed in the region of 1645 and 3100–3600 cm^{-1} corresponding to $CaCl_2$ and between at 600–660, 1400–1600 and 3400–3500 cm^{-1}, indicating the presence of sulphate characteristic peaks. Sulphates were more and dominantly influenced the TiO_2 particles surface with the increasing concentration of the treatment, whereas the functional groups of $CaCl_2$ interacted with the surface of TiO_2 particles with the lowest concentration of the treatment. The surface functionality with the treatment of $CaCO_3$ + $CaSO_4$ indicated that the associated peaks of $CaCO_3$ and $CaSO_4$ characterized the 0.01 and 0.1 M of the treatment (figure 1f). The peaks between 1400 and 1600 cm^{-1} correspond to the sulphate characteristics appearing with the lowest concentration treatment of the combination of $CaCO_3$ + $CaSO_4$. The triple impacts of the Ca compounds was also characterized with FTIR and the spectrum indicated the presence of functional groups for all three Ca compounds (figure 1g). Similar with the other spectrums, the functional groups that originated from the Ca compounds were identified on the surface with the treatment of 0.01 and 0.1 M of Ca treatment. However, characteristics of sulphate-related peaks between 1400 and 1600 cm^{-1} clearly identified with the lowest concentration of the treatment. This is an indication that the TiO_2 particles can be modified by the interaction of various Ca compounds. In this interaction, the anionic part of the Ca compounds also influenced the surface functionality and the anionic part has potential to attach to the particle surface according to Ca compounds concentration.

To understand and compare the surface interactions between TiO_2 nanoparticles and individual and combined presence of Ca compounds, the crystallinity and functional group indices of TiO_2 particles were also evaluated, as they indicate the surface deformation/formation. The crystallinity significantly decreased with the tested Ca compounds compared with the control (figure 2a). No concentration dependency was found with the treatment of $CaCl_2$ and $CaSO_4$ + $CaCl_2$. However, there was significant concentration dependency with $CaCO_3$, $CaCO_3$ + $CaCl_2$, $CaCO_3$ + $CaSO_4$ and $CaCO_3$ + $CaSO_4$ + $CaCl_2$, where increasing concentrations of Ca decreased the crystallinity. As shown in figure 2a, the highest decrease in the crystallinity obtained with the existence of $CaCO_3$. In contrast, increasing the concentration of Ca as $CaSO_4$ increased the crystallinity. The results showed that the occurrence of CO_3^{2-} deformed the surface of TiO_2 particles rather than other Ca compounds. On the other hand, $CaCl_2$ might limit the concentration dependence behaviour. The results also showed that the only possible factor by the $CaCl_2$ on the impact of the crystallinity is the Ca part of $CaCl_2$, since the anionic part of $CaCl_2$, which is Cl, can have potential to limit changes on the crystallinity. It can be originated that the heteroatoms, like Cl, can limit the interaction with the surface of TiO_2 particles [37]. On the other hand, Ca compounds such as CO_3^{2-} and SO_4^{2-} includes non-heteroatoms, their interactions can contribute to the particle crystallinity and the surface deformation of the TiO_2 particles [38].

Figure 3 shows the functional group indices of control and treated TiO_2 particles with various Ca compounds. The results of hydroxyl indices indicated that there were no significant differences upon treatment with $CaCO_3$ and $CaCO_3$ + $CaSO_4$. However, the hydroxyl indices significantly decreased at high concentrations of $CaCl_2$, $CaSO_4$, $CaCO_3$ + $CaCl_2$, $CaSO_4$ + $CaCl_2$ and $CaCO_3$ + $CaSO_4$ + $CaCl_2$, which indicates the formation of hydroxyl groups. Moreover, it shows concentration dependency. Wang *et al* [39] examined the TiO_2 nanoparticles by sol–gel process to increase surface hydroxyl groups and improve photocatalytic activity in the presence of NaCl, and addition of NaCl increased the hydroxyl groups in the surface. Similarly, in our study, presence of $CaCl_2$ and $CaSO_4$ increased the hydroxyl groups on the surface of TiO_2 nanoparticles with

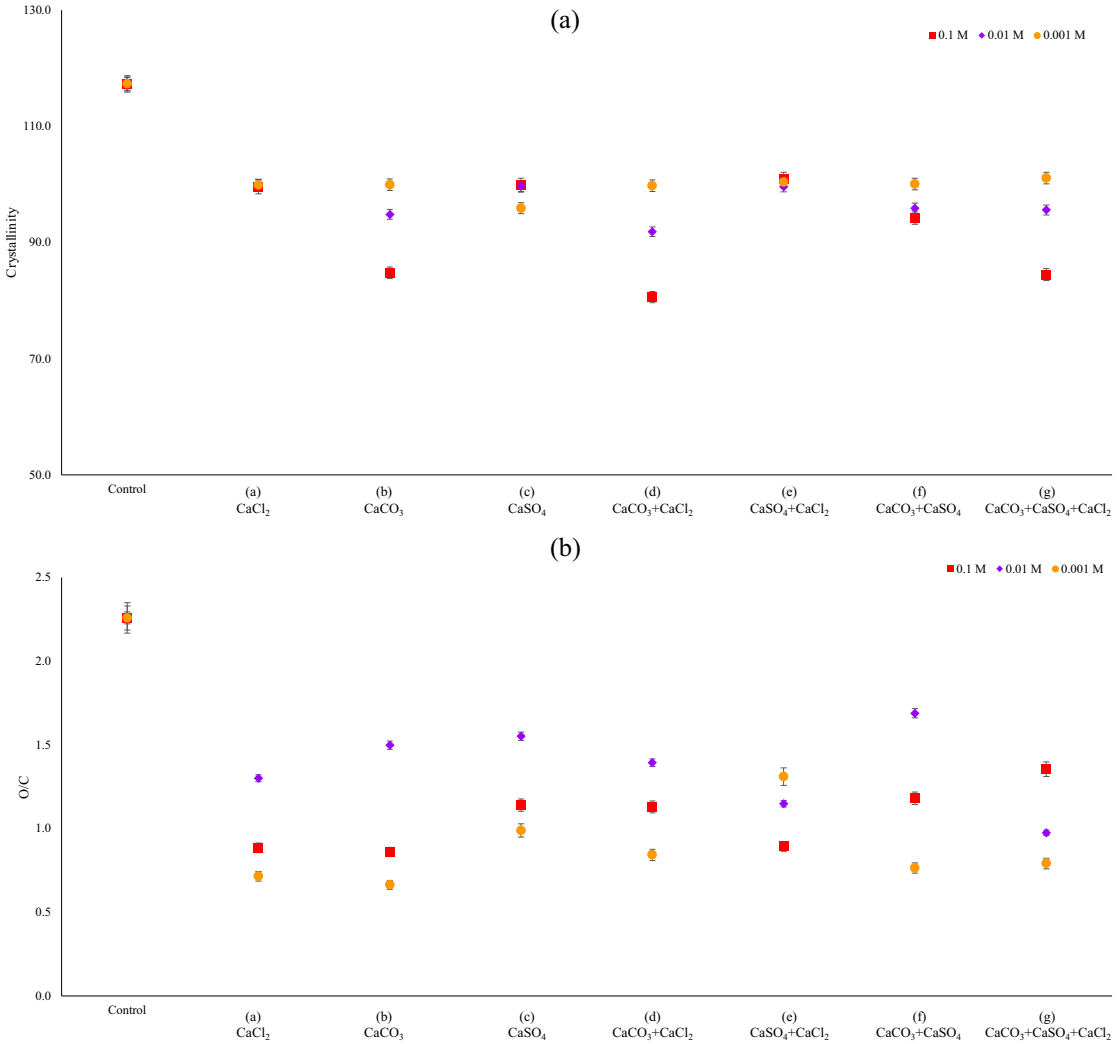

Figure 2. (**a**) Crystallinity and (**b**) O/C of TiO_2 particles treated with various Ca compounds using various concentrations. The FTIR and EDX spectra used for the crystallinity and O/C calculation, respectively.

increasing concentration of Ca compounds. The highest formation obtained with presence of $CaCl_2$ compared to the presence of $CaSO_4$. Although $CaCl_2$ and $CaSO_4$ influence the hydroxyl group formation, the results also showed that treatment with $CaCO_3$ does not affect hydroxyl group formation on the surface of TiO_2 nanoparticles. These results also suggested that the presence of $CaCO_3$ did not influence the surface deformation by the hydroxylation compared to the other Ca compounds.

The carbonyl indices are also depicted in figure 3. The results showed no significant decreases in the carbonyl index, except at a high concentration treatment of $CaCl_2$, $CaCO_3 + CaCl_2$, and $CaSO_4 + CaCl_2$. This result indicated that the occurrence of higher concentration of Ca by $CaCl_2$ has also potential to form new carbonyl groups, which can unstabilize the hydrophilicity of the particles and cannot protect the surface for carbonyl deformation.

Figure 3 illustrates the effect of Ca compounds on the vinyl groups of TiO_2 particles. The vinyl indices significantly increased upon treatment with Ca compounds. The decrease in the vinyl groups has potential to decline hydrophobicity of the particles, as hydrophobicity is the association of nonpolar groups in an aqueous environment [40]. However, concentration dependency was not observed in all cases. This result might show that the anionic part of the Ca compounds has limitedly influenced on the formation of vinyl groups on TiO_2 particles, except $CaSO_4$.

EDX analysis revealed the elemental composition of TiO_2 particles with the treatment of various Ca compounds as well as distribution of co-occurring elements with the different Ca treatments (figure 4 and supplementary table 2). It was observed that untreated TiO_2 particles were nearly 5% and contained other elements. It is probable that the synthesis method of the TiO_2 particles included these chemicals [41]. In the meantime, the percentage of TiO_2 particles were changed with the Ca treatments. The EDX results also approved that some contaminants in the untreated TiO_2 nanoparticles, such as N, Na, Zn, were

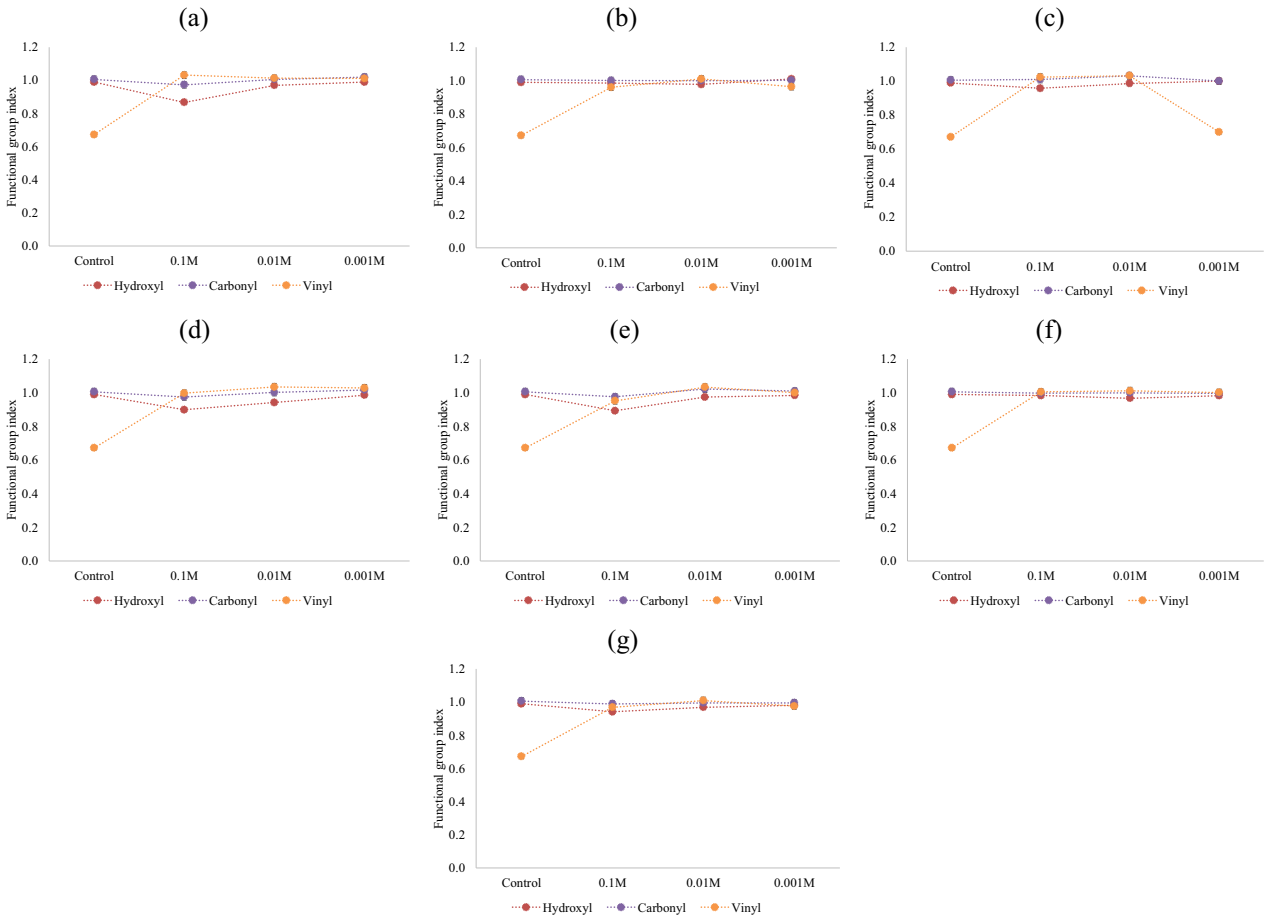

Figure 3. Functional (hydroxyl, carbonyl and vinyl) group indices of TiO_2 particles treated with individual and combined Ca compounds using various concentrations. The treatments are indicated as (**a**) $CaCl_2$, (**b**) $CaCO_3$, (**c**) $CaSO_4$ and their combinations (**d**) $CaCO_3 + CaCl_2$, (**e**) $CaSO_4 + CaCl_2$, (**f**) $CaCO_3 + CaSO_4$, (**g**) $CaCO_3 + CaSO_4 + CaCl_2$.

removed by the Ca treatments and the highest relative Ti content was obtained at the 0.01 M treatments of Ca, except the treatment of $CaSO_4 + CaCl_2$ and $CaCO_3 + CaSO_4 + CaCl_2$. The spectra showed Ca identified on the Ti surface with the 0.01 M treatments of Ca compounds, except individual treatment of $CaSO_4$ and $CaCl_2$. Moreover, anionic part of the Ca compounds, such as S and Cl, was identified at the highest concentration of the treatment in all cases. The attachment of the inorganic ligands (e.g., CO_3^{2-}, Cl^- and S^{2-}) suggested that they may have to influence on the complexation of metal ions, and stabilization of metal oxide particles [23]. Besides, the results were in good agreements with the FTIR spectra (figure 1). To evaluate the impact of the Ca compound treatments on the surface oxidation state and backbone of the TiO_2 particles, the O/C was calculated and the results are illustrated in figure 2b. These results indicated that the O/C significantly decreased with the Ca compound treatments and lower O/C showed that the photocatalytic activity was limited by the Ca treatment compared to control. Moreover, the O/C order of the individual treatment of Ca compounds by the concentration were 0.01 M > 0.1 M > 0.001 M. The higher O/C ratio at 0.01 M of Ca treatment can be originated that the carbonyl, peroxide or alcohol related groups on the surface are more representative in this concentration [42]. Another explanation can be the functionalization of the particles by Ca compounds. The functionalization of the particles can affect its carbon backbone, and occurrences of other anions can lead to loss of carbon from the particle phase. Therefore, staged oxidation levels may be obtained. In the double combination of Ca compounds, the trend of O/C was similar with individual Ca treatments in the treatment of $CaCO_3 + CaCl_2$ and $CaCO_3 + CaSO_4$, on the other hand, the O/C was decreased with increasing concentration of the treatment of $CaSO_4 + CaCl_2$, whereas the O/C increased with the increasing concentration of triple concentration of Ca compounds. This result indicated that the combination of Ca compound influenced the oxidation of TiO_2 backbone.

The co-occurrence of the ligands in Ca compounds can alter the aggregation and stability of the nanoparticles. The interaction between various Ca compounds and TiO_2 particles was also examined through the zeta potentials and particle sizes of TiO_2 particles. Figure 5 shows the zeta potentials and particle size of TiO_2 nanoparticles treated

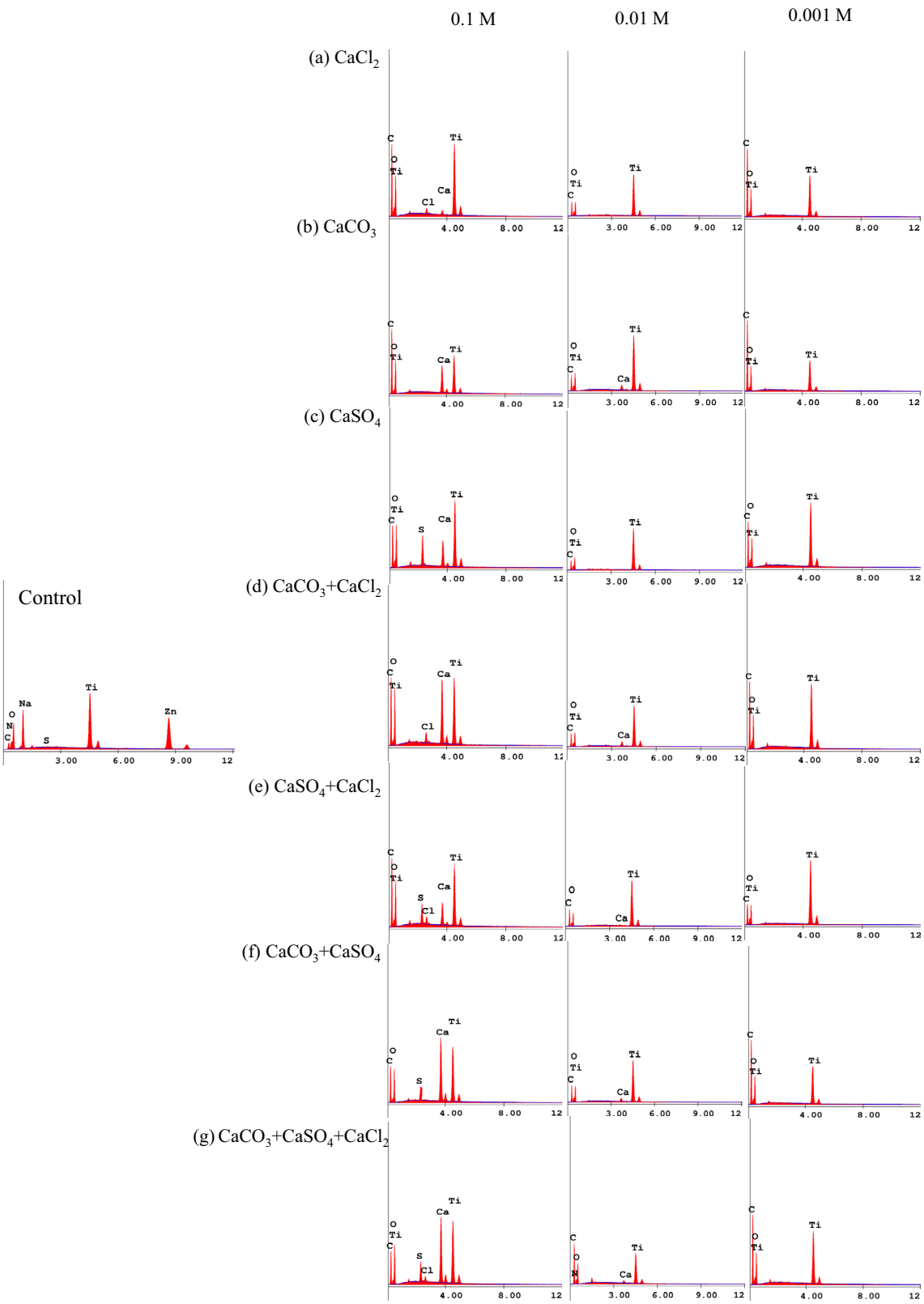

Figure 4. EDX spectra of TiO_2 particles treated with individual and combined Ca compounds using various concentrations. The treatments are indicated as (**a**) $CaCl_2$, (**b**) $CaCO_3$, (**c**) $CaSO_4$ and their combinations (**d**) $CaCO_3 + CaCl_2$, (**e**) $CaSO_4 + CaCl_2$, (**f**) $CaCO_3 + CaSO_4$, (**g**) $CaCO_3 + CaSO_4 + CaCl_2$.

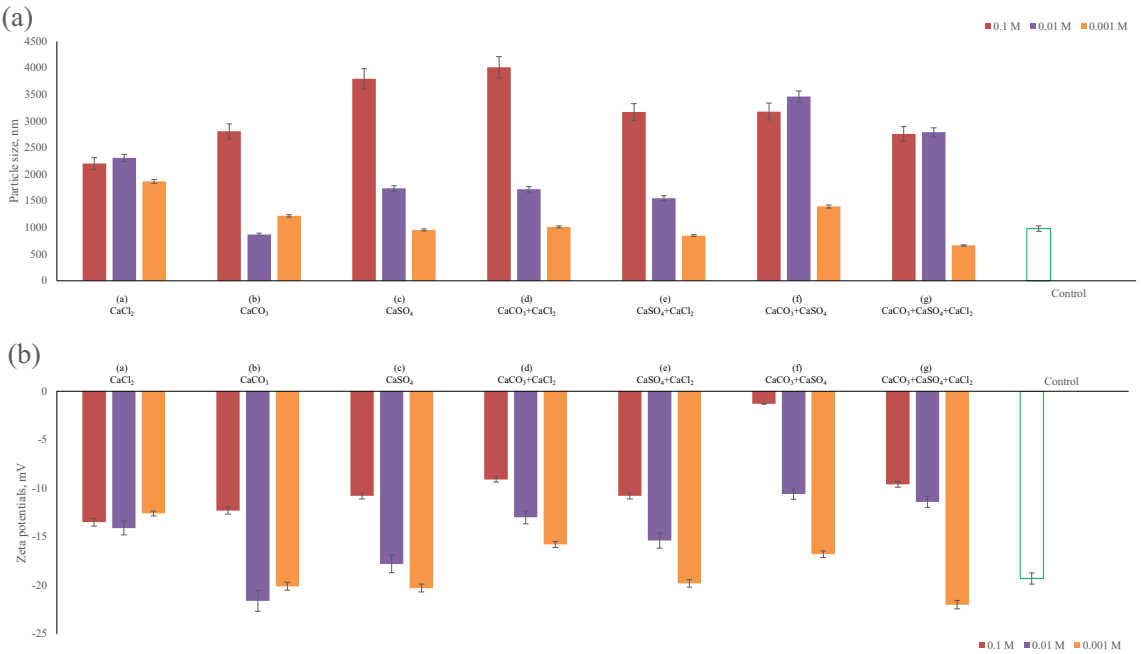

Figure 5. (**a**) Particle size and (**b**) zeta potentials of TiO_2 particles treated with individual and combined Ca compounds using various concentrations.

with various Ca compounds. The results indicated that the zeta potentials and particle sizes of TiO_2 particles were significantly influenced by the Ca compounds compared to its control. The zeta potentials indicated the concentration dependency and the highest zeta potentials obtained at the treatment of the lowest concentration of the Ca compounds, which indicates the stability of the particles. This might be that the lowest concentration of the treatments cleaned the surface impurities, which affected the surface stability. However, with the increasing treatment concentration, the introduction of the new functional groups on the surface might cause the loss of stabilization on the particles and the negativity of the zeta potentials decreased compared to control and the treatments at lower concentrations. Additionally, as expected, the particle sizes were negatively correlated with zeta potentials, except individual treatment of $CaCl_2$. The higher particle sizes obtained with the increasing treatment concentrations. This result is also in a good agreement with the SEM images (supplementary figure 1).

The relation between surface characteristics and the zeta potentials were also evaluated, and the results showed that the crystallinity and zeta potentials of TiO_2 particles treated with $CaCl_2$, $CaCO_3$, $CaCO_3 + CaCl_2$, $CaCO_3 + CaSO_4$ and $CaCO_3 + CaSO_4 + CaCl_2$ had a strong positive correlation (r:0.811, r:0.789, r:0.742 and r:0.846 for $CaCl_2$, $CaCO_3$, $CaCO_3 + CaCl_2$, $CaCO_3 + CaSO_4$ and $CaCO_3 + CaSO_4 + CaCl_2$, respectively). The vinyl groups also significantly negatively affected the zeta potentials of TiO_2 particles treated with $CaCO_3$ (r:0.723) and $CaSO_4$ (r:0.804). Moreover, both the hydroxyl groups had strong negative correlations with the zeta potentials of $CaCO_3 + CaCl_2$ (r:0.761), $CaSO_4 + CaCl_2$ (r:0.803) and $CaCO_3 + CaSO_4 + CaCl_2$ (r:0.748). On the one hand, the O/C of TiO_2 treated with $CaCl_2$ (r:0.827), $CaCO_3$ (r:0.671) and $CaSO_4 + CaCl_2$ (r:0.801) and their zeta potentials had positive correlation, while on the other hand, the zeta potentials of the TiO_2 treated with $CaCO_3 + CaSO_4 + CaCl_2$ had negative correlation with its O/C (r:0.754).

4. Conclusion

To our knowledge, this is the first study that evaluates the role of individual and combined Ca compounds on the surface chemistry of TiO_2 nanoparticles by mimicking the environmental or aqueous applications. This study confirmed that the surface of TiO_2 nanoparticles significantly transformed in the presence of various Ca compounds. This transformation was dependent on the type of Ca compound, their combinations and concentrations. The results showed that the increasing concentration of individual and combined presence of Ca compounds triggered the agglomeration, while in some cases the zeta potentials increased. In these processes, both surface deformation and formation have influenced on TiO_2 nanoparticles. As illustrated in the supplementary figures 2–8, each conditions induced the transformation with different surface characteristics. For example, all Ca compounds and their combinations had no effect on the carbonyl groups and decreased the vinyl groups. Moreover, individual $CaCl_2$ protected the surface by the crystallinity and reduction of hydroxyl groups

compared to the individual forms of CO_3^{2-} and SO_4^{2-}. Additionally, individual $CaCO_3$ have potential to protect the surface oxidation of TiO_2 by hydroxylation. However, their combinations changed the characteristics of TiO_2 particles. With these results, we have demonstrated here the high dependency of experimental conditions in surface characteristics of TiO_2 particles and how the presence of compounds and their forms and concentrations can modify the nanoparticles profile.

References

[1] Naasz S, Altenburger R and Kühnel D 2018 *Sci. Total Environ.* **635** 1170

[2] Sun Q, Hu X, Zheng S, Sun Z, Liu S and Li H 2015 *Powder Technol.* **274** 88

[3] Baysal A and Saygin H 2020 *Smart nanosensors and methods for detection of nanoparticles and their potential toxicity in air, in nanomaterials for air remediation* (Elsevier) p 33

[4] Baysal A, Saygin H and Ustabasi G S 2020 *Environ. Monit. Assess.* **192** 1

[5] Baysal A, Saygin H and Ustabasi G S 2020 *Environ. Monit. Assess.* **192** 276

[6] Baysal A, Saygin H and Ustabasi G S 2018 *Environ. Monit. Assess.* **190** 34

[7] Baysal A, Saygin H and Ustabasi G S 2018 *Arch. Environ. Prot.* **44** 85

[8] Baysal A, Saygin H and Ustabasi G S 2018 *Environ. Health Eng. Manag.* **6** 73

[9] Baysal A and Saygin H 2019 *Environ. Eng. Manag. J.* **18** 2683

[10] Horie M, Nishio K, Fujita K, Endoh S, Miyauchi A, Saito Y *et al* 2009 *Chem. Res. Toxicol.* **22** 543

[11] Le Ouay B and Stellacci F 2015 *Nano Today* **10** 339

[12] Li M, Lin D and Zhu L 2013 *Environ. Pollut.* **173** 97

[13] Liu X, Wazne M, Chou T, Xiao R and Xu S 2011 *Water Res.* **45** 105

[14] Han Y, Kim D, Hwang G, Lee B, Eom I, Kim P J *et al* 2014 *Colloids Surf. A Physicochem. Eng. Asp.* **451** 7

[15] Peng Y H, Tsai Y C, Hsiung C E, Lin Y H and Shih Y H 2017 *J. Hazard. Mater.* **322** 348

[16] Dong H and Lo I M 2013 *Water Res.* **47** 2489

[17] Zhang F, Wang Z, Wang S, Fang H and Wang D 2019 *Chemosphere* **228** 195

[18] Tan L, Tan X, Fang M, Yu Z and Wang X 2018 *J. Mol. Liq.* **264** 261

[19] Baalousha M, Nur Y, Römer I, Tejamaya M and Lead J R 2013 *Sci. Total Environ.* **454–455** 119

[20] Hogan C M 2010 in A Jorgensen and C Cleveland (eds) *Encyclopedia of Earth* National Council for Science and the Environment, Washington DC p 1

[21] Millero F J, Feistel R, Wright D G and McDougall T J 2008 *Deep-Sea Res.* **55** 50

[22] Bundschuh M, Filser J, Lüderwald S, McKee M S, Metreveli G, Schaumann G E *et al* 2018 *Environ. Sci. Eur.* **30** 6

[23] Deng R, Lin D, Zhu L, Majumdar S, White J C, Gardea-Torresdey J L *et al* 2017 *Nanotoxicology* **11** 591

[24] Juganson K, Ivask A, Blinova I, Mortimer M and Kahru A 2015 *Beilstein J. Nanotechnol.* **6** 1788

[25] Petersen E J 2015 *NIST Special Publication* 1200

[26] Petersen E J, Henry T B, Zhao J, MacCuspie R, Kirschling T L, Dobrovolskaia M A *et al* 2014 *Environ. Sci. Technol.* **48** 4226

[27] Holden P A, Gardea-Torresdey J L, Klaessig F, Turco R F, Mortimer M, Hund-Rinke K *et al* 2016 *Environ. Sci. Technol.* **50** 6124

[28] Selck H, Handy R D, Fernandes T F, Klaine S J and Petersen E J 2016 *Environ. Toxicol. Chem.* **35** 1055

[29] Forest V 2021 *NanoImpact* **23** 100344

[30] Sanchís J, Olmos M, Vincent P, Farré M and Barceló D 2016 *Environ. Sci. Technol.* **50** 961

[31] Lü X, Xia B, Liu C, Yang Y and Tang H 2016 *J. Nanomater.* **2016** 8735620

[32] Ahumada M, Lazurko C and Alarcon E I 2019 in Julia Pérez Prieto, María González Béjar (eds) *Micro and nano technologies, photoactive ınorganic nanoparticles* (Elsevier) p 1

[33] Brandon J, Goldstein M and Ohman M D 2016 *Pollut. Bull.* **110** 299

[34] Stark N M and Matuana L M 2004 *Polym. Degrad. Stab.* **86** 1

[35] Saygin H and Baysal A 2021 *J. Polym. Environ.* **29** 958

[36] Irshad M A, Nawaz R, Zia ur Rehman M, Imran M, Ahmad J, Ahmad S *et al* 2020 *Chemosphere* **258** 127352

[37] Sethy N K, Arif Z, Mishra P K and Kumar P 2020 *Green Process. Synth.* **9** 171

[38] Campisi S, Chan-Thaw C E and Villa A 2018 *Appl. Sci.* **8** 1159

[39] Wang J, Liu X, Li R, Qiao P, Xiao L and Fan J 2012 *Catal. Commun.* **19** 96

[40] Caron G, Ermondi G and Scherrer R A 2007 in B Testa and H van de Waterbeemd (eds) *Comprehensive medicinal chemistry II* (Oxford: Elsevier) p 425

[41] Castro A L, Nunes M R, Carvalho A P, Costa F M and Florencio M H 2008 *Solid State Sci.* **10** 602

[42] Tua P, Hall I V W A and Johnston M V 2016 *Anal. Chem.* **19** 4495